




Probability weighted moments regularization based blind image De-blurring

Hussain Dawood¹  · Hassan Dawood² · Guo Ping³ · Rashid Mehmood⁴ · Ali Daud⁵ · Abdullah Alamri⁶ · Jalal S. Alowibdi⁶

Received: 31 August 2018 / Revised: 26 February 2019 / Accepted: 18 March 2019/

Published online: 4 April 2019

© Springer Science+Business Media, LLC, part of Springer Nature 2019

Abstract

The main objective of blind image de-blurring is to recover a sharp image from a given blurry image. A good estimation of the kernel plays an important role in recovering a sharp image. However, if the local object textures are neglected when the kernel is being estimated, this can lead to over-smoothing or can produce a strong ringing effect. In this paper, a new image regularization term based on the Probability Weighted Moments (PWM) for kernel estimation is proposed named as Probability Weighted Moments Regularization (PWMR). PWMR has the ability to preserve the small local texture structure in an image while minimizing the artifacts. Further, it can preserve the better contrast information between neighboring pixels and their corresponding central pixels in a current sliding window; moreover, it has the ability to resist outliers even in a small sample size. The kernel estimated by PWMR is subsequently used to recover the sharp latent image. An extensive comparison of synthetic and real standard benchmark images indicates the effectiveness of PWMR compared to current state-of-the-art blind image de-blurring methods.

Keywords Blind image de-blurring · Image regularization · Kernel estimation · Probability weighted moments

1 Introduction

Digital imaging has enabled people to save memorable moments in their lives. However, when they are being captured, images can be contaminated by various effects such as noise [34], blurring [6, 13, 15, 17, 21, 28–31, 34, 36], hazing [24, 25], fogging [26], barcode de-blurring [22] and sequential ocular images from multi-spectral imaging [16] etc. These undesirable effects may occur for a number of reasons; for example, camera movement while the picture is being taken is a common problem that can produce a blurred image. Based on the characteristics, image de-

✉ Hussain Dawood
hdaoud@uj.edu.sa

blurring algorithms are mainly divided into two types. In first type of image de-blurring, the blur kernel is known. In the second type, the blur kernel is unknown; this is known as blind image de-blurring. In this paper, we focus on blind image de-blurring and, more specifically, on kernel estimation. The estimated kernel can be further used with any image de-blurring method to recover an image.

There are two phases to blind image de-blurring: 1) kernel estimation, and 2) image de-blurring. Both phases play an equally important role in the recovery of a clear image. Kernel estimation is an effective means of dealing with a blurred image. The better the estimation of the kernel, the better will be the recovered image., blind image de-blurring has attained the researchers' attention. Blind image de-blurring has been successfully applied in different fields such as audio signal processing, astronomical and medical image processing.

Based on different properties, kernel estimation techniques are broadly categorized into two types: (1) Variational Bayes (VB) [6, 13, 28, 29] and (2) Maximum A Posterior (MAP) [3, 15, 17, 21, 23, 30, 31, 34, 36]. VB-based methods have the ability to evade trivial solutions; however, the computational cost is higher compared to MAP. Two variants have been proposed to estimate the kernel based on MAP: (1) Kernel estimation achieved by using the salient structures of an object is known as Salient Structures-Based Kernel Estimation [2, 3, 12, 17, 23, 30, 36] and (2) Sparse Regularization-Based Kernel Estimation [9, 11, 15, 21, 31, 34, 35]. The main focus of this paper is on the second type of MAP-based image de-blurring method.

Earlier, single image de-blurring did not perform well because of kernel priors and different latent variables [3, 30]. Although researchers used Gaussian priors, the estimated kernels were not able to preserve the structures of salient objects and did not provide compact, sparse representation. This led to a noise-contaminated image with dense structures. Salient edges are detected from a gradient image by the use of l_1 -norm [2]. Image priors obtained in this way can produce better results only under certain conditions [2, 15, 21]. To improve the quality of the image, a combination of l_1 -norm and a new ring suppressing term was employed [23]. To suppress the small structures, l_1/l_2 -norm regularization term was introduced [11] where a l_1 to l_2 norm ratio was applied to high frequencies of an image. This regularization term was unable to produce images with sharp edges, as the ratio of the l_1 to l_2 does not have this property.

A new method for generalized sparse representation for uniform and non-uniform motion de-blurring was proposed by [31]. Here, the authors mathematically proved the soundness of l_0 -norm for sparse representation. Moreover, the proposed system requires fewer iterations to converge the system because no extra filtering is needed during the optimization process. However, the proposed technique did not perform well on real images containing text.

To handle the outlier, a new effective kernel estimation method was proposed which considered the data fidelity term to suppress the effect of outliers [7]. The estimated kernel was further used to recover the degraded image. However, the computational cost increased due to outlier detection. Row-Column sparsity has been used for blind image de-blurring [18]. Authors proposed to solve a new type of sparsity optimization problem by including rows and columns to estimate the kernel. Singular value decomposition was used to recover the kernel and latent image from the blurred image.

To remove the noise and recover the blurred image, a new inverse Radon transform-based kernel was estimated [34]. Multiple directional filters with different orientations were applied to the input image and a true Radon transform was estimated for each image. However, multiple directional filters produced significant ringing artifacts in the recovered images. To preserve the smooth structure of an object for blind image de-blurring, an iteration-wise generalized shrinkage–threshold method was proposed [36]. Here, the authors extended the

generalized shrinkage–thresholding (GST) that is used to sharpen the salient edges of an object while eliminating the small details. However, the elimination of small details can lead to an inaccurate estimation of the blind kernel.

A single-image blind de-blurring based on the color image priors has been proposed to better preserve the sharp edges of an object [12]. The normalized color line was used to estimate the blur kernel instead of the original color line that is not effective for estimation. A method was proposed for the selection of effective centroids, which was more effective compared to K-means method. A new generalized MAP-estimation framework for blind image de-blurring was proposed [35], in which the scene specific edge priors were used. Dark channel image priors were proposed by [9] who assumed that the dark channel image priors are less sparse.

The salient structure of an image plays an important role in estimating the kernel. Most of the existing methods neglect the small texture structures when estimating the kernel for convolution with the image. The neglect of such structures can lead to the problem of over-smoothed edges of an object within the image. Better contrast information gives a more accurate estimation of the blurred kernel. Two well-known approaches are used to determine the contrast of an image: maximum likelihood estimation (MLE) and probability weighted moments (PWM). PWM has the proven ability to provide better contrast information while preserving the edges of an object even for a small sample size as compared to MLE which is further used for image classification [4].

This paper presents an effective image regularization method whereby a new type of image regularization approach is introduced that recovers sharp images from blurry images. The kernel estimated by using the PWMR has the ability to preserve the trivial structures that are further used to recover the image. This allows an extremely cost-effective formulation to be used for the blind de-convolution model, consequently obviating the need for additional methods. The salient contributions of this work are as follows:

- a) New image regularization term by utilizing the PWM to preserve the small textures of an object which helps to recover an improved, sharper image.
- b) The proposed PWMR has the ability to identify the outliers and disregard them during the estimation of the kernel, and also reduces the ringing effect with comparable computational cost.

2 Background knowledge

In this section, a brief introduction to PWM is presented.

2.1 Probability weighted moments

PWM has the ability to uniquely determine the distribution of given data. MLE can be used to capture the tails of distribution, which can affect the estimation because the tails or ending points may be the outliers. However, the PWM can be used to better capture the middle of the distribution, thereby providing a better estimation of given data.

Below is a better linear estimate of standard deviation for the normal distribution [5]:

$$PWM = \frac{\sqrt{\pi}}{n} \sum_{i=1}^n \left[X_i - 2 \left(1 - \frac{i-0.5}{n} \right) X_i \right]$$

where X_i refers to the ordered observations within the sample of size n . The estimation of the standard deviation using PWM is also a function of ordered observations. The expression $(i - 0.5)/n$ denotes the empirical distribution function; π is 3.1416.

PWM has been successfully applied in different fields for better estimation such as in image classification [4], in Heteroscedastic Linear Regression Model for adaptive estimation [20] and estimation for the better-quality control charts [19].

3 Probability weighted moments based regularization

PWM as the linear function of the sample space has less influence on the sample variability. PWM renders a better estimation of the parameters compared to the conventional moments in the presence of outliers within the sample space. The closed form of a cumulative distribution function provides unbiased, stable and particularly attractive PWM. This property improves our estimation of the blind kernel for recovering the corrupted image.

The local relationships among the textures of image objects are investigated to estimate the blind kernel named PWM-based Regularization (PWMR). More precisely, each pixel is considered to estimate the kernel by utilizing efficient and effective PWMR defined as follows:

$$PWMR = \frac{PWM_x}{PWM_y},$$

Where PWM_x refers to the estimated variance in the direction of x derivate, and PWM_y denotes the estimated variance in the direction of y derivate. As PWM are less sensitive to the outliers when considering the coefficient in the direction of the x -axis, and the y -axis has the ability to preserve the salient edges of an object. The terms PWM_x and PWM_y in the equation above provide the horizontal and vertical structures in a given blurred image. The ratio of these terms provides the compact value of a given structure which is neither a noisy value nor the motion blur caused due to motion. Different regularization techniques have been proposed to find the best estimate of a kernel. However, neglecting the small salient regions by considering the outliers/ noise does not produce the better kernel which can then be used recover the latent image. Most of regularization techniques approach the problem as a non-convex problem, which needs an optimization technique to solve it.

4 Proposed framework

Commonly, image de-blurring models are defined as follows:

$$y = kx + n,$$

Where y is the obtained blurred image, n is the additive Gaussian i.i.d noise, x and k denote the unknown sharp image and blurring matrix used to blur the sharp image x , respectively. Blind image de-blurring is considered to be a greatly ill-posed inverse problem, in which there is a need to estimate the sharp image x and the blurring matrix

k , simultaneously The blind image de-blurring algorithm is mainly divided into two parts: unknown kernel estimation and image de-blurring. A better estimation of the unknown kernel can improve the quality of the recovered image. A standard blind image de-blurring is presented in Algorithm 1.

Algorithm 1 (complete image de-blurring algorithm)

Input: Blurry image I , maximum size of kernel to estimate ker_h

Output: Obtained sharp Image x (Recovered image)

(The proposed algorithm is mainly divided into two stages)

1. Estimate the Blind kernel matrix k form high frequency image I (Obtained by applying the derivative to blurred image y).
 Estimate the blind kernel using subsection A
 Alternatively obtain the coarse-to-fine x and k in loop
 - a. Update the high frequency image x by using the proposed PWMR
 - b. Update the blurring (kernel) matrix k by using Section 4-A
 Repeat till the finer version of x and k is obtained.
2. Recover the de-blurred image by non-blind method
 Recover the sharp image x , using the estimated kernel k on blurred image I .

A. Kernel Estimation

Kernel estimation is accomplished for the high frequency of an image as in [11]. High frequency image I is obtained from the blurry image, which is actually the combination of derivatives in the x and y direction. More precisely, the following filters are used to obtain the high frequency images in horizontal (x -axis) and vertical (y -axis) directions as,

$$\nabla_x = [1, -1]; \quad \nabla_y = [1, -1]^T.$$

Where ∇_x filter used in horizontal direction, and ∇_y filter used in vertical direction (which is the transpose (T) of ∇_x). The de-blurring model can be defined as

$$\min_{x,k} \lambda \|x \otimes k - I\|_2^2 + PWMR + \beta \|k\|_1 \tag{1}$$

Where k and x represent the unknown kernel and sharp image, respectively. PWMR is the proposed regularization term for image de-blurring, λ and β are the trade-off parameters used to optimize the stability of kernel and image regularization terms, and is the 2D convolution operator. l_1 -norm as regularization term is applied on k to reduce the noise during the kernel estimation which also presents a good, sparse representation. In consideration of the physical principles for blur formation, k is bounded by two restrictions: $k \geq 0$ and $\sum_i k_i = 1$. Due to the high convexibility of Eq. 1, in order to optimize the solution, an initialization is assumed on both x and k ; after that, x and k are alternatively updated. To update x and k , the altering method suggested by [11] is employed.

To update x and k , Eq. 1 can be divided into two parts as follows:

$$\min_{x,k} \lambda \|x \otimes k - I\|_2^2 + PWMR \tag{2}$$

$$\min_{x,k} \lambda \|x \otimes k - I\|_2^2 + \beta \|k\|_1 \tag{3}$$

The new term, PWMR, in Eq. 2 makes it a convex problem. The Iterative Shrinkage-Thresholding Algorithm (ISTA) [1] is used to solve the general linear inverse problem. The algorithm applied to update x is presented as follows:

Algorithm for updating x

Input: Image x obtained from previous stage, Blur kernel matrix k obtained from previous stage, the regularization parameter λ , high frequency image I , require number of maximum outer iterations M , and maximum number of inner iterations N

Output: Image x^M

```

for i=1: M
 $\lambda^i = \lambda \|x^j\|_2$ 
 $x^{i+1} = \text{ISTA}(k, \lambda^i, x^i, t, N)$ 
end M
The ISTA algorithm is presented as follows
for j=1: N
 $d = I - tk^T(kx^j - I)$ 
 $x^{j+1} = S_{t\lambda}(d)$ 
end N
output Image  $x^N$ 
    
```

Where k is the blurring matrix obtained after last iteration of k and $t = 0.001$ is the threshold value used for ISTA. M and N denote the maximum number of inner and outer iterations, respectively and considered as 2 in the proposed algorithm. S represents the vector soft shrinkage operator to decrease the input vector towards zero as presented in Eq. 4.

$$S_x(x)_i = \max(|x_i| - \alpha, 0) \text{sign}(x_i) \tag{4}$$

The ISTA algorithm is used for the inner iteration updating of x , and the outer iteration is used only for the re-estimation of the likelihood term in eq. 2.

It is necessary to update k after updating x by using eq. 3. An unconstrained Iterative Re-weighted Least Squares method [14] is used to estimate the kernel by using the weights obtained from the previous updated matrix of k (with single outer iteration). The estimated kernel may have negligible values at the finest level, which are normalized to zero to enhance the efficiency of obtained kernel against noise. Coarse-to-fine pyramid of image resolutions is used for the multi-scale estimation of the kernel.

B. Image De-blurring

Once the fine kernel has been obtained, any non-blind image de-blurring algorithm can be used to recover the sharp image [10, 14]. A fast image de-convolution algorithm is used to recover the sharp image, which employs Hyper-Laplacian priors after the estimated kernel has been obtained. The underlying algorithm [10] is robust against small kernel errors, and is as follows:

$$\min_x \lambda \|x \otimes k - I\|_2^2 + \|\nabla_x\|_b + \|\nabla_y\|_b$$

Where ∇_x and ∇_y are the derivative filters used aforesaid section A. Where $b = 0.8$ and $\lambda = 3000$ as in [11]. Non-blind de-convolution is far lower ill-posed problem as compared to blind de-convolution. Therefore, in the current scenario, a l_p -type regularization term is used to solve the aforementioned cost function as defined in [10].

5 Results and discussion

To validate the effectiveness of the proposed method, results are obtained for both synthetic and real-world images with well-known performance measures. This section is further subdivided into three sub-sections: performance measures, experimental results, and discussion of the synthetic dataset and real-world images.

5.1 Performance measure

The performance of the PWMR method was evaluated using well-known performance measures: Peak signal to Noise Ratio (PSNR), Structural Similarity Index Measure (SSIM), Error ratio, and time in seconds. The PSNR was obtained with

$$PSNR = 10 \cdot \log_{10} \left(\frac{MAX^2}{MSE} \right)$$

Where ' MAX ' represents the maximum possible value present in an image. ' MSE ' is the mean squared error between the original image (pure image) ' O ' and restored image ' R ' as follows:

$$MSE = \left(\frac{1}{M \times N} \right) \sum_{i=1}^M \sum_{j=1}^N (O-R)^2$$

$M \times N$ is the size of the original and restored image, where ' M ' is the total number of rows and ' N ' is the total number of columns. The similarity structure between the original image and restored image is obtained by Structural Similarity Index method (SSIM) as follows:

$$SSIM = \frac{(2\mu_O\mu_R + c_1)(2\sigma_{OR} + c_2)}{(\mu_O^2 + \mu_R^2)(\sigma_O^2 + \sigma_R^2 + c_2)}$$

Where ' c_1 ' and ' c_2 ' are constant values. ' μ_O ', ' μ_R ', ' σ_O ', ' σ_R ' and ' σ_{OR} ' represent the means, variances and co-variances. The subscript 'o' and 'r' represents the original and restored images, respectively. The error ratio is defined as follows:

$$r_{error} = std(I_{EK}, I_R) / std(I_{RK}, I_R)$$

I_{EK} and I_{RK} represents the image recovered by using the estimated kernel and true kernel respectively. I_R shows the real image and $std()$ is the standard deviation.

Table 1 Comparison of Levin et al.'s dataset (Levin et al. [15]) using Mean PSNR, SSIM, computational time (In seconds) and Error Ratio

Method/ Image	PSNR	SSIM	Time	Error ratio
Known k	32.32	0.9385	–	1.0000
Levin et al. [15]	28.73	0.8916	80.5917	1.5531
Krishnan et al. [11]	28.22	0.8586	10.1178	2.1369
Cho and Lee [3]	28.87	0.8845	2.3942	1.4082
Xu et al. [30]	29.41	0.9000	2.9371	1.4071
Jinsha et al. [9]	30.87	0.9203	28.37	1.1934
Yue et al. [32]	30.1332	0.9119	12.7206	1.2198
PWMR	30.14	0.9122	25.1276	1.2271

5.2 Synthetic data

A well-known standard benchmark dataset [15] for synthetic images was used to evaluate the PWMR against other state-of-the-art methods. In all experiments, the same images were used to validate the effectiveness of the PWMR. This dataset contained four 255×255 images as well as eight different blur kernels varying in size from 13×13 to 27×27 . After convolving the kernels with the images, a total of 32 images were obtained. The given dataset contained the blurry images, ground-truth kernels and ground-truth images.

Table 1 shows a detailed comparison of the synthetic dataset provided by [15]. The results of PWMR are compared in terms of PSNR, SSIM, computational time and the error ratio with baselines [3, 9, 11, 15, 30, 32]. PWMR outperforms existing methods in terms of PSNR and

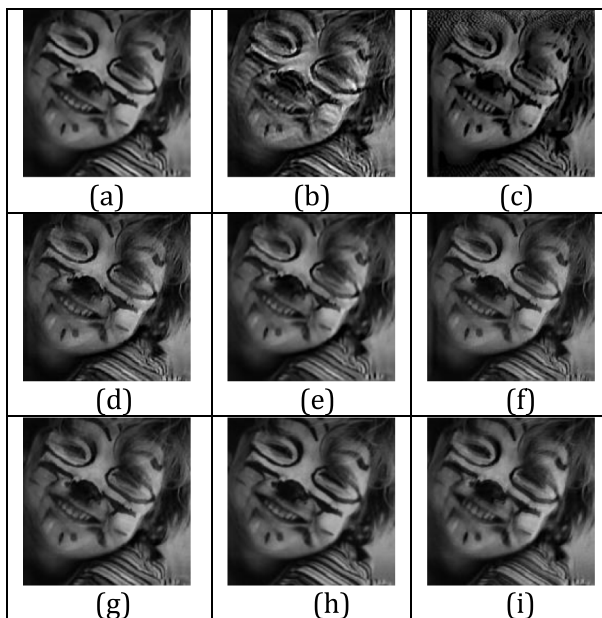


Fig. 1 Example of de-blurring results for Levin et al. [15] (27×27 Kernel size.) (a) Original image, (b) image recovered by Shan et al. [23], (c) Cho and Lee [3], (d) Xu et al. [30], (e) Levin et al. [13], (f) Xu et al. [31], (g) Perrone et al. [21], (h) Jinsha et al. [9] and (i) PWMR

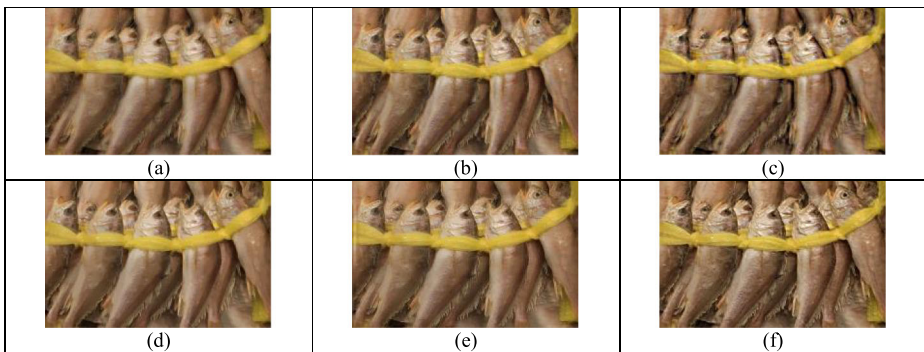


Fig. 2 Visual results for the fish image (a) image recovered by Whyte et al. [27], (b) image recovered by Xu et al. [31], (c) image recovered by Zhang et al. [33] (d) image recovered by Jinsha et al. [9], (e) image recovered by Zuo et al. [36], (f) image recovered by PWMR

SSIM except for [9]. However, the computational cost of [9] is little higher than PWMR. The capability of PWMR to preserve the small texture while estimating the kernel gives a better reconstruction of an image.

Figure 1 depicts the visual comparison of results between PWMR and other state-of-the-art methods on dataset given by [15] for one image. Visual evaluation indicates that the kernel estimated by employing PWMR has comparable results with other methods [3, 9, 13, 21, 23, 30, 31]. The image recovered by PWMR has better visualization except for [9, 21]. The dark image prior with sparsity preserves the edges better than PWMR. However, PWMR is faster than [9]. The image recovered by [23] has strong ringing effects and is still somewhat blurred compared to the image recovered by [3].

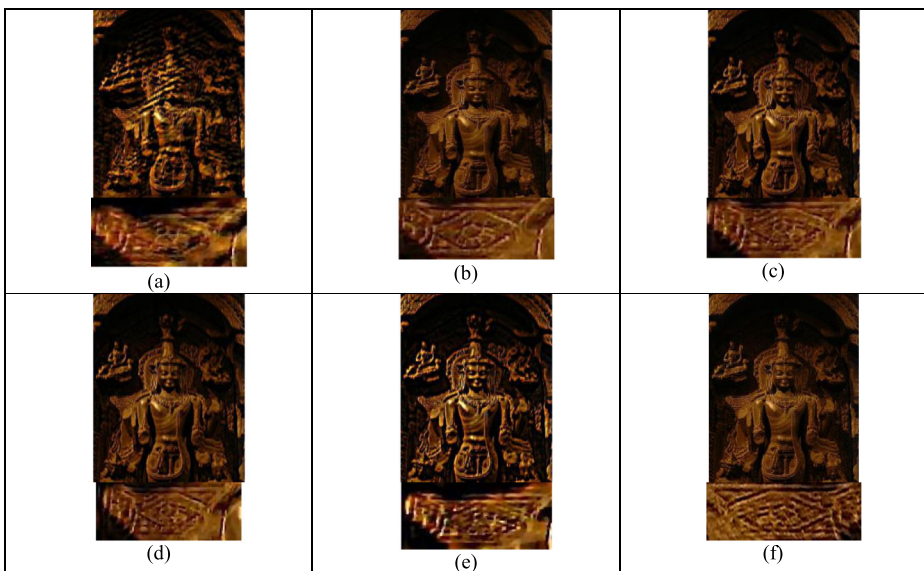


Fig. 3 Visual results on Lyndsey image. Image recovered by (a) Fergus et al. [6], (b) Xu et al. [30] (c) Krishnan et al. [11], (d) Zhang et al. [28] (e) Perrone et al. [21] (f) PWMR

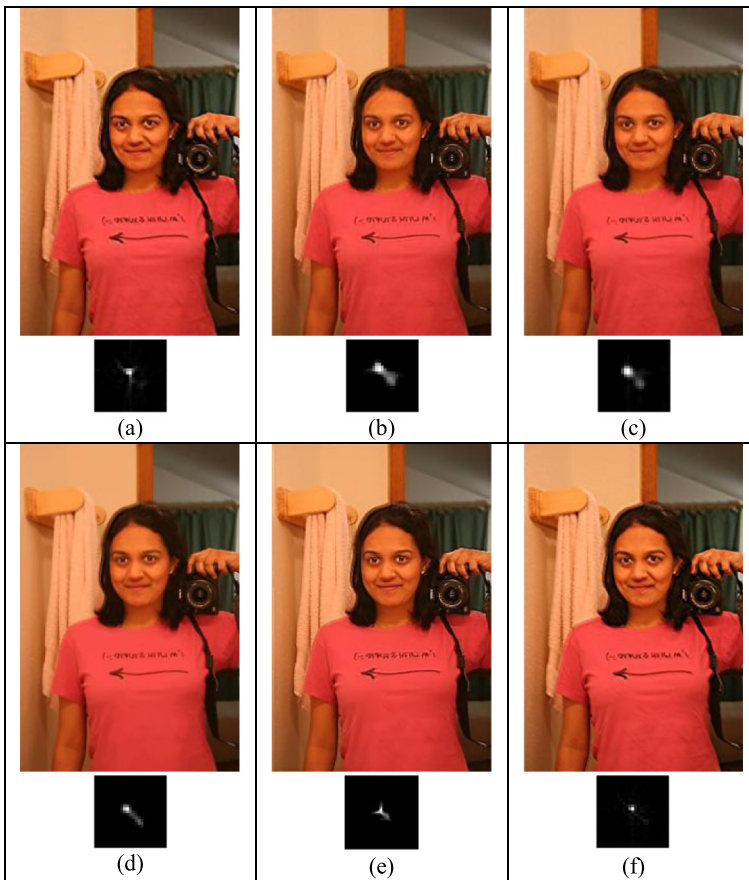


Fig. 4 Visual results for Mukta image also showing the estimated kernel. Image recovered by (a) Krishnan et al. [11] (b) Zhong et al. [34], (c) Michaeli et al. [17], (d) Jinsha et al. [8], (e) Zuo et al. [36], (f) PWMR

5.3 Real-world images

Real-world standard images are also evaluated in order to compare the proposed regularization method with state-of-the-art methods. The real-world images have no ground truth, enabling them to be compared visually. To ensure a fair comparison, we have used all methods with their proposed parameters.

Figure 2 depicts the comparison of PWMR with [9, 27, 31, 33, 36] for a real-world image of fish. Although images recovered by the methods proposed by [9, 31, 36] are somewhat fine, the recovered images have over-smoothened the local texture of the object. Therefore, the local geometry of objects has not been preserved. The image recovered by [33] is over-sharp and the ringing effect on the image is amplified. Similarly, the image recovered by [27] has a strong ringing effect. PWMR has less ringing effect compared to that produced by state-of-the-art methods, and also better preserves the fine textures during the removal of the blur.

Figure 3 presents the results for the Lyndsey image (with the zoomed area of an image to show the effectiveness of image de-blurring methods) of PWMR with [6, 11, 21, 28, 30]. The zoomed area of an image recovered by PWMR preserved the small texture structures

compared to results produced by the aforementioned methods. The image recovered by other methods either over-smoothed [11, 28, 30] or increased the contrast [21] with a strong ringing effect. It is also clear that image recovered by [6] still has a strong ringing effect.

Figure 4 shows the visual results for the Mukta image as well as the kernel recovered by Michaeli et al. [17], Zhong et al. [34], Zuo et al. [36], Krishnan et al. [11], Jinsha et al. [8] and PWMR. The visual images of the recovered kernels shows the effectiveness of PWMR compared with the kernels recovered by other methods. The kernel recovered by PWMR is less sparse and the neighboring pixels are more compact, which can help to recover a better image during the convolution process while preserving a better texture. The image recovered by Zuo et al. [36] produced a strong ringing effect and also increased the contrast of the image. The image recovered by Jinsha et al. [38] neglected the small texture during image recovery, causing an over-smoothed image.

6 Conclusion

An efficient and effective image regularization term based on Probability Weighted Moments is proposed as a means of estimating kernel function for blind image de-blurring. It is concluded that PWM has the ability to preserve the small textures regardless of the outliers in a small sample space. One can also see that the kernel estimated by using the proposed PWMR has the ability to restore the edges of objects much better and with less ringing effect compared to other methods. The effectiveness of PMWR on synthetic and real-world images, in terms of visually plausible de-blurring, PSNR, SSIM, Error ratio and computational cost has been confirmed.

For the future, when restoring an image, a better estimation of kernel can be considered while taking into the global and local textures of the image.

Acknowledgements This work is fully supported by the grants from the Joint Re-search Fund in Astronomy (Grant No. U1531242) under cooperative agreement between the National Natural Science Foundation of China (NSFC) and Chinese Academy of Sciences (CAS), Prof. Ping Guo is the author to whom all correspondence should be addressed.

References

1. Beck, A.; Teboulle, M.: A fast iterative shrinkage- thresholding algorithm for linear inverse problems. *SIAM J Imag Sci*, 2, pp. 183–202(2009)
2. Chanand TF, Wong C-K (1998) Total variation blind deconvolution. *IEEE Trans Image Process* 7:370–375
3. Cho S.; and Lee, S.: Fast motion deblurring. In *ACM Trans Graph (TOG)*, 28, p. 145(2009)
4. Dawood H, Dawood H, Guo P (2012) Combining the contrast information with WLD for texture classification. *IEEE Int Conf Comput Sci Auto Eng (CSAE) 2012*:203–207
5. Downton F (1966) Linear estimates with polynomial coefficients. *Biometrika* 53:129–141
6. Fergus R, Singh B, Hertzmann A, Roweis ST, Freeman WT (2006) Removing camera shake from a single photograph. *ACM Trans Graphics (TOG)* 25:787–794
7. Jiangxin D, Pan J, Su Z, Yang M (2017) Blind image deblurring with outlier handling. *Proc IEEE Conf Comput Vision Pattern Recogn IEEE Conf Comput Vision Pattern Recogn (CVPR) 2017*:2478–2486
8. Jinsha P, Deqing S, Hanspeter P, Hsuan YM (2016) Blind image deblurring using dark channel prior. *IEEE Conf Comput Vision Pattern Recogn (CVPR) 2016*:1628–1636
9. Jinsha P, Deqing S, Hanspeter P, Hsuan YM (2017) Deblurring images via Dark Channel prior. *IEEE Trans Pattern Anal Mach Intell (PAMI)*
10. Krishnan D, Fergus R (2009) Fast image deconvolution using hyper-Laplacian priors. *Adv Neural Inform Process Syst (NIPS) 2009*:1033–1041

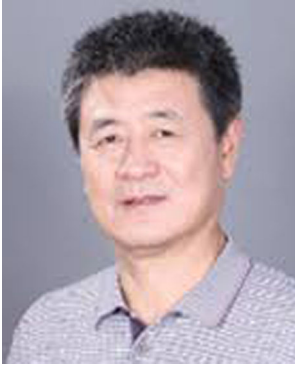
11. Krishnan D, Tay T, Fergus R (2011) Blind deconvolution using a normalized sparsity measure. *IEEE Conf Comput Vision Pattern Recogn (CVPR)* 2011:233–240
12. Lai WS, Ding JJ, Lin YY, Chuang YY (2015) Blur kernel estimation using normalized color-line priors. *IEEE Conf Comput Vision Pattern Recogn (CVPR)* 2015:64–72
13. Levin A, Weiss Y (2011) F. Durand, Freeman, W. T.: efficient marginal likelihood optimization in blind deconvolution. *IEEE Conf Comput Vision Pattern Recogn (CVPR)* 2011:2657–2664
14. Levin A, Fergus R, Durand F, Freeman W (2007) Image and depth from a conventional camera with a coded aperture. *ACM Trans Graph (TOG)* 26:70
15. Levin A, Weiss L, Durand F, Freeman WT (2009) Understanding and evaluating blind deconvolution algorithms. *IEEE Conf Comput Vision Pattern Recogn (CVPR)* 2009:1964–1971
16. Lian J, Zheng Y, Jiao W, Yan F, Zhao B (2018) Deblurring sequential ocular images from multi-spectral imaging (MSI) via mutual information. *Med Biol Eng Comput* 56(6):1107–1113
17. Michaeli T, Irani M (2014) Blind deblurring using internal patch recurrence. *Eur Conf Comput Vision (ECCV)* 2014:783–798
18. Mohammad T, Li Y, Monga V (2018) Blind image Deblurring using row-column sparse representations. *IEEE Signal Process Lett (SPL)* 25:273–278
19. Muhammad F, Riaz M (2006) Probability weighted moments approach to quality control charts. *Econ Qual Contrl* 21:251–260
20. Muhammad F, Aslam M, Pasha GR (2008) Adaptive estimation of heteroscedastic linear regression model using probability weighted moments. *J Mod Appl Stat Methods* 7:15
21. Perrone D, Favaro P (2014) Total variation blind deconvolution: the devil is in the details. *IEEE Conf Comput Vision Pattern Recogn (CVPR)* 2014:2909–2916
22. Pu H, Fan M, Yang J, Lian J (2018) Quick response barcode deblurring via doubly convolutional neural network. *Multimed Tools Appl*, pp.1–16
23. Shan Q, Jia J, Agarwala A (2008) High-quality motion deblurring from a single image. *ACM Trans Graph (TOG)* 27:73
24. Singh D, Kumar V (2017) Modified gain intervention filter based dehazing technique. *J Modern Optics (JMO)* 64:2165–2178
25. Singh D, Kumar V (2017) Dehazing of remote sensing images using fourth-order partial differential equations based trilateral filter. *IET Comput Vis*
26. Singh D, Kumar V (2018) Defogging of road images using gain coefficient-based trilateral filter. *J Electron Imag* 27:013004
27. Whyte O, Sivic J, Zisserman A, Ponce J (2012) Non-uniform deblurring for shaken images. *Int J Comput Vision (IJCV)* 98:168–186
28. Wipf D, Zhang H (2013) Analysis of Bayesian blind deconvolution. *Int Workshop Energy Minim Meth Comput Vision Pattern Recogn* 2013:40–53
29. Wipf D, Zhang H (2014) Revisiting bayesian blind deconvolution. *J Mach Learn Res*: 3595–3634
30. Xu L, Jia L (2010) Two-phase kernel estimation for robust motion deblurring. In *European Conference on Computer Vision (ECCV)* 2010:157–170
31. Xu L, Zheng S, Jia J (2013) Unnatural l_0 sparse representation for natural image deblurring. *IEEE Conf Comput Vision Pattern Recogn (CVPR)* 2013:1107–1114
32. Yue T, Cho S, Wang J, Dai Q (2014) Hybrid image deblurring by fusing edge and power spectrum information. *Eur Conf Comput Vision (ECCV)* 2014:79–93
33. Zhang H, Wipf D, Zhang Y (2013) Multi-image blind deblurring using a coupled adaptive sparse prior. *IEEE Conf Comput Vision Pattern Recogn (CVPR)* 2013:1051–1058
34. Zhong DL, Cho S, Metaxas D, Paris S, Wang J (2013) Handling noise in single image deblurring using directional filters. *IEEE Conf Comput Vision Pattern Recogn (CVPR)* 2013:612–619
35. Zhou Y, Komodakis N (2014) A map-estimation framework for blind deblurring using high-level edge priors. *Eur Conf Comput Vision (ECCV)* 2014:142–157
36. Zuo W-M, Dongwei R, David Z, Shuhang G, Lei Z (2016) Learning iteration-wise generalized shrinkage–thresholding operators for blind deconvolution. *IEEE Trans Image Process (TIP)* 25:1751–1764



Hussain Dawood received his MS and PhD degree in Computer Application Technology from Beijing Normal University, Beijing, china in 2012 and 2015, respectively. He is currently working as an Assistant Professor at College of Computer Science and Engineering, University of Jeddah, Jeddah, Saudi Arabia. His current research interests include image processing, pattern recognition, and Computer Vision.



Hassan Dawood is currently working as an Assistant Professor at Department of Software Engineering, University of Engineering and Technology, Taxila, Pakistan. His research interests include image restoration, feature extraction and image classification. He has received his MS and PhD degree in Computer Application Technology from Beijing Normal University, Beijing, china in 2012, and 2015, respectively.



Ping Guo (IEEE Senior Member) is currently a professor at School of Systems Science, Beijing Normal University, and the School of Computer Science and Technology of Beijing Institute of Technology. From 1993 to 1994 he was with the Department of Computer Science and Engineering at the Wright State University as a visiting faculty. From May 2000 to August 2000 he was with the National Laboratory of Pattern Recognition at Chinese Academy of Sciences as a guest researcher. He is the author or co-author of more than 200 papers. His current research interests include neural network, pattern recognition, image processing, software reliability engineering, optical computing, and spectra analysis.



Rashid Mehmood has received his Ph. D from Beijing Normal University, Beijing China. Currently he is working as postdoc researcher at Karolinska Institute, Sweden at the department of cancer and cell biology. He is affiliated with University of kotli, AJ&K Pakistan and working there as Assistant Professor. His current research interest includes genetics and cancer research, machine learning, image processing, data mining, and computational biology.



Ali Daud obtained his Ph.D. degree from Tsinghua University (July 2010). He is Associate Professor and head of Data Mining and Information Retrieval Group, IIU, Islamabad, Pakistan. He has published about 70 papers in reputed international Impact Factor journals and conferences. He has taken part in many research projects and is Principal Investigator (PI) of two projects. His research interests include Data Mining, Social Network Analysis and Mining, Probabilistic Models, Scientometrics, and Natural Language Processing.



Abdullah Alamri received his B.S. degree in Computer Science from King Khalid University, Saudi Arabia in 2007, and received M.S. degree in Information Technology from School of Engineering & Mathematical Sciences, La Trobe University, Australia in 2009 and his Ph.D. in Computer Science from RMIT University, Australia in 2014. He is currently working as an Assistant Professor with the College of Computer Science and Engineering, University of Jeddah, Jeddah, Saudi Arabia. His research interests include Big Data, Internet of Things, Database Systems and Semantic Web.



Jalal Alowibdi is a faculty member in the College of Computer Science and Engineering at University of Jeddah. Alowibdi completed his Ph.D. in Computer Science at the University of Illinois at Chicago, his Master's degree in Software Engineering from DePaul University. He is working on various complex problems in Data Mining and Privacy in Social Networks. Recently, he has focused on Image Processing, Data Mining, Privacy in Social Networks and Information Retrieval. Currently, Alowibdi is the Chair of the Department of Computer Science and the director of the center of the Information Technology at the University of Jeddah. Also, He is the Deputy Director of Web Observatory research center at King Abdulaziz University.

Affiliations

Hussain Dawood¹ • **Hassan Dawood**² • **Guo Ping**³ • **Rashid Mehmood**⁴ • **Ali Daud**⁵ • **Abdullah Alamri**⁶ • **Jalal S. Alowibdi**⁶

Hassan Dawood
hasandawod@yahoo.com

Guo Ping
pguo@ieee.org

Rashid Mehmood
gulkhan007@gmail.com

Ali Daud
ali.daud@iiu.edu.pk

Abdullah Alamri
amalamri@uj.edu.sa

Jalal S. Alowibdi
jalowibdi@uj.edu.sa

¹ Department of Computer and Network Engineering, College of Computer Science and Engineering, University of Jeddah, Jeddah, Saudi Arabia

² Department of Software Engineering, University of Engineering and Technology, Taxila, Pakistan

³ School of Systems Science, Beijing Normal University, Beijing, People's Republic of China

⁴ Department of Software Engineering, University of Kotli, Azad and Jammu Kashmir, Pakistan

⁵ Department of Computer Science & Software Engineering, International Islamic University, Islamabad, Pakistan

⁶ College of Computer Science and Engineering, University of Jeddah, Jeddah, Saudi Arabia